

# Investigation of Anisotropy on Deterioration of Mechanical Parameters of Layered Rock Under Freeze-thaw Cycles

**Guangkeng Zhang**

Central South University School of Geosciences and Info Physics <https://orcid.org/0000-0002-1209-656X>

**Lianrong Wu**

Yunn Diqing Nonferrous Metals Co.,Ltd.

**Huiyun Wang**

Kunming Survey and Design Institute of China Nonferrous Metals Industry

**Zhipeng Li**

Yunn Diqing Nonferrous Metals Co.,Ltd.

**Baosheng Shi**

Yunn Diqing Nonferrous Metals Co.,Ltd.

**Qingxi Wei**

Kunming Survey and Design Institute of China Nonferrous Metals Industry

**Chengzhi Xia**

Central South University School of Geosciences and Info Physics

**Guangyin Lu** (✉ [1207973174@qq.com](mailto:1207973174@qq.com))

Central South University School of Geosciences and Info Physics

---

## Research Article

**Keywords:** layered rock, freeze-thaw cycle, bedding dip, mechanical parameters, deformation characteristics of the slope, slope stability

**Posted Date:** August 3rd, 2021

**DOI:** <https://doi.org/10.21203/rs.3.rs-645506/v1>

**License:** © ⓘ This work is licensed under a Creative Commons Attribution 4.0 International License.

[Read Full License](#)

---

# Investigation of anisotropy on deterioration of mechanical parameters of layered rock under freeze-thaw cycles

Guangkeng Zhang<sup>1,2</sup> · Lianrong Wu<sup>3</sup> · Huiyun Wang<sup>4</sup> · Zhipeng Li<sup>3</sup> · Baosheng Shi<sup>3</sup> · Qingxi Wei<sup>4</sup> · Chengzhi Xia<sup>1,2</sup> · Guangyin Lu<sup>1,2,\*</sup>

<sup>1</sup> School of Geosciences and Info-Physics, Central South University, Changsha 410083, China; zgk2019@csu.edu.cn (Guangkeng Zhang); xiachengzhi@csu.edu.cn (Chengzhi Xia)

<sup>2</sup> Key Laboratory of Metallogenic Prediction of Nonferrous Metals and Geological Environment Monitoring Ministry of Education, Central South University, Changsha 410083, China;

<sup>3</sup> Yunn Diqing Nonferrous Metals Co., Ltd., Diqing 474400, China; 195011071@csu.edu.cn (Lianrong Wu); dj195011068@csu.edu.cn (Zhipeng Li); 195012169@csu.edu.cn (Baosheng shi)

<sup>4</sup> Kunming Survey and Design Institute of China Nonferrous Metals Industry, Kunming 650000, China; wuyang98@csu.edu.cn (Huiyun Wang); liang.zhang@csu.edu.cn (Qingxi Wei)

Correspondence should be addressed to Guangyin Lu; luguangyin@csu.edu.cn

## Abstract

The evaluation of slope deformation and stability under freeze-thaw cycles is an important research direction and a challenge for geotechnical engineering in cold regions. However, most previous studies only considered the influence of the number of freeze-thaw cycles, but ignored the anisotropic characteristics of layered rock slopes. Meanwhile, the number of freeze-thaw cycles and the bedding dip are rarely considered in previous numerical simulations. Based on this background, the carbonaceous slate of the Pulang copper mine in China was used as the sample material to perform uniaxial compression tests on seven types of carbonaceous slate with different bedding dip angles after completing six different times of freeze-thaw cycles. The test results are applied to the numerical simulation analysis of the deformation characteristics and stability of the layered rock slope of the copper mine. The results show that freezing and thawing will cause layered rock degradation effects, thereby reducing rock mechanical parameters, and the influence is most obvious when the bedding dip is approximately 45°. In the numerical simulation, it is found that the deformation characteristics and stability change trend of the layered rock slope are similar to the above-mentioned experiments. In addition, it is necessary to consider the number of freeze-thaw cycles and the bedding dip to avoid too much difference for the maximum horizontal displacement of a layered rock slope. This study provides a feasible evaluation plan for the deformation characteristics and stability of the layered rock slope in Pulang area of China.

**Keywords:** layered rock · freeze-thaw cycle · bedding dip · mechanical parameters · deformation characteristics of the slope · slope stability

## Introduction

Due to seasonal climate changes, rocks in cold regions are often damaged by freezing and thawing effects, bringing hidden dangers to humans. Freeze-thaw effects can cause rock deformation, landslides and other hazards (Yan et al. 2015). This kind of continuous damage to rocks has been considered by

scholars who have studied it as a factor related to the occurrence of disasters (Arosio et al. 2013; Zwissler et al. 2014). With the development of geotechnical engineering and the increasing exploration of mineral resources in cold regions, accurate assessment of the stability of rock slopes and control of the risk of freezing and thawing have become an important topic (Li et al. 2001; Wu and Liu 2005). The study of rock mechanics parameters of freeze-thaw cycles provides important data for stability analysis of rock slopes and reduction of freeze-thaw hazards.

At present, many scholars have carried out a large number of studies on the changes in mechanical properties of rocks during freezing and thawing cycles. Chen et al. (2019) studied the degradation mechanism of quartz sandstone in Tianshan Highway after freeze-thaw cycles through laboratory mechanical tests. The results showed that the freeze-thaw cycles changed the microstructure of quartz sandstone and weakened its mechanical properties. And on the basis of experimental phenomena, a new constitutive model was established to reflect the changes in the mechanical properties of the rock during the freeze-thaw cycle and predict the deformation of the rock mass. Li et al. (2021) used NMR porosity and volumetric strain to define rock freeze-thaw and creep damage factors to study the characteristics of rock damage under long-term freeze-thaw cycles and loads. They found that as the freeze-thaw cycles increase, rock Viscosity parameters will decrease rapidly, causing continuous damage and continuous decrease in strength of the rock. Wen et al. (2014) used granite and porphyry as freeze-thaw test materials, calculated the safety factors of granite and porphyry before and after the freeze-thaw cycle, compared them, and analyzed the influence of freeze-thaw on the slope. Korshunov et al. (2016) et al. used numerical simulation methods to evaluate the influence of freeze-thaw cycles on slope stability. The results showed that when the slope is thawed, the safety factor will decrease from 2.15 to 1.13. Qiao et al. (2015) established a rock mechanical property evaluation and prediction system, and applied the system to the evaluation of rock slope stability, and analyzed the adaptability of Urumqi-Yulin highway slope under freeze-thaw cycles. Ismail and Mustafa (2016) established a predictive model through uniaxial compression tests after freeze-thaw cycles to analyze the deterioration of the uniaxial compressive strength of rock cores caused by freeze-thaw cycles. However, many scholars often regard rocks as isotropic in freezing and thawing experiments. Rocks such as slate are stratified, which are characterized by the same physical and mechanical properties in the isotropic plane, but in the direction perpendicular to this plane. However, the physical and mechanical properties are quite different (Chen et al. 2016, Mokhtari et al. 2016). Therefore, the influence of bedding dip angle should be considered in the freeze-thaw test. At present, scholars have determined the relationship between elastic modulus, Poisson's ratio and shear modulus and the bedding dip angle through a series of uniaxial and triaxial compression tests (Amadei 1996). Tien and Kuo (2001) et al. found through experiments that with the distribution of bedding inclination, the uniaxial compressive strength will show different changes. Fu et al (2019) conducted uniaxial compression tests on seven different bedding inclination angles after different freeze-thaw cycles, established and verified a new uniaxial compression strength prediction model through experimental data, and analyzed different layers The influence of physical dip and freeze-thaw cycles on the elastic parameters and uniaxial compressive strength of slate. The above experimental studies have proved that the bedding dip has a significant influence on the elastic parameters and compressive strength of the rock.

Therefore, this article chooses carbonaceous slate from the Pulang copper mine in Yunnan, China as the sample material to study the effects of the number of freeze-thaw cycles and bedding dip on the elastic modulus, poisson's ratio and uniaxial compressive strength of carbonaceous slate. And analyzed the degradation mechanism of rocks under freezing conditions. Elastic constitutive equations and test

methods are used to calculate the physical parameters of rock masses. Combining the experimental results with the carbonaceous slate slope of the Pulang copper mine in Shangri-La, Yunnan, China, the finite element software is used to simulate and calculate the deformation characteristics and stability of the carbonaceous slate slope with different bedding dips after freezing and thawing cycles.

## Experimental test method

### Elastic constitutive equation

According to the generalized Hooke's law, the stress-strain relationship of the local rectangular coordinates  $x'$   $y'$   $z'$  of slate can be expressed as

$$\begin{bmatrix} \varepsilon_{x'} \\ \varepsilon_{y'} \\ \varepsilon_{z'} \\ \gamma_{x'y'} \\ \gamma_{y'z'} \\ \gamma_{z'x'} \end{bmatrix} = [S'] \{\sigma'\} = \begin{bmatrix} \frac{1}{E_1} & -\frac{\mu_1}{E_1} & -\frac{\mu_2}{E_2} \\ -\frac{\mu_1}{E_1} & \frac{1}{E_1} & -\frac{\mu_2}{E_2} \\ -\frac{\mu_2}{E_2} & -\frac{\mu_2}{E_2} & \frac{1}{E_2} \\ & & & \frac{2(1+\mu_1)}{E_1} \\ & & & & \frac{1}{G_2} \\ & & & & & \frac{1}{G_2} \end{bmatrix} \begin{bmatrix} \sigma_{x'} \\ \sigma_{y'} \\ \sigma_{z'} \\ \tau_{x'y'} \\ \tau_{y'z'} \\ \tau_{z'x'} \end{bmatrix} \quad (1)$$

Where  $\alpha$  is the bedding dip angle and five independent elastic constants of  $E_1, \mu_1, E_2, \mu_2$  and  $G_2$ : the elastic modulus and Poisson's ratio of  $E_1$  and  $\mu_1$  in the direction parallel to the bedding dip angle, and the elasticity of  $E_2, \mu_2$  The modulus and poisson's ratio are respectively perpendicular to the bedding dip surface.

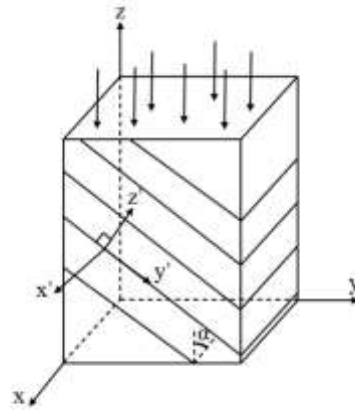


**Fig. 1** Three-dimensional coordinate transform model of slate

As shown in Figure 1, according to the principle of coordinate transformation and the local

rectangular coordinates are mapped to  $\alpha$  counterclockwise around the  $x'$  axis, the stress-strain relationship corresponding to the global rectangular coordinate  $xyz$  is

$$\{\varepsilon\} = [S]\{\sigma\} \quad (2)$$

Where  $\{\varepsilon\}$ ,  $\{\sigma\}$  and  $[S]$  are the strain matrix, stress matrix and flexibility matrix corresponding to the global rectangular coordinates  $xyz$ , respectively. The flexibility matrix can be calculated as follows:

$$[S] = [Q]^T [S'] [Q] \quad (3)$$

Where  $[Q]$  is the coordinate transformation matrix of elastic parameters, which can be expressed as follows:

$$[Q] = \begin{bmatrix} 1 & 0 & 0 & 0 & 0 & 0 \\ 0 & \cos^2 \alpha & \sin^2 \alpha & 0 & -\sin 2\alpha & 0 \\ 0 & \sin^2 \alpha & \cos^2 \alpha & 0 & \sin 2\alpha & 0 \\ 0 & 0 & 0 & \cos \alpha & 0 & \sin 2\alpha \\ 0 & \frac{\sin 2\alpha}{2} & -\frac{\sin 2\alpha}{2} & 0 & \cos 2\alpha & 0 \\ 0 & 0 & 0 & \sin \alpha & 0 & -\cos \alpha \end{bmatrix} \quad (4)$$

Substituting equations (3) and (4) into equation (2), the stress-strain relationship corresponding to the global rectangular coordinate  $xyz$  can be obtained as follows:

$$\begin{bmatrix} \varepsilon_x \\ \varepsilon_y \\ \varepsilon_z \\ \gamma_{xy} \\ \gamma_{yz} \\ \gamma_{zx} \end{bmatrix} = \begin{bmatrix} S_{11} & S_{12} & S_{13} & 0 & S_{15} & 0 \\ S_{12} & S_{22} & S_{23} & 0 & S_{25} & 0 \\ S_{13} & S_{23} & S_{33} & 0 & S_{35} & 0 \\ 0 & 0 & 0 & S_{44} & 0 & S_{46} \\ S_{15} & S_{25} & S_{35} & 0 & S_{55} & 0 \\ 0 & 0 & 0 & S_{46} & 0 & S_{66} \end{bmatrix} \bullet \begin{bmatrix} \sigma_x \\ \sigma_y \\ \sigma_z \\ \tau_{xy} \\ \tau_{yz} \\ \tau_{zx} \end{bmatrix} \quad (5)$$

Given that the uniaxial compression test is used to obtain the five elastic parameters of slate, the axial stress indicates  $\sigma_z \neq 0$  in the stress matrix  $\{\sigma\}$ . Therefore, the flexibility matrix  $[S]$  only provides the values of  $S_{13}$ ,  $S_{23}$ ,  $S_{33}$  and  $S_{35}$ . These values can be calculated as follows:

$$\begin{aligned} S_{13} &= -\frac{\mu_1}{E_1} \sin^2 \alpha - \frac{\mu_2}{E_2} \cos^2 \alpha, \\ S_{23} &= -\frac{\mu_2}{E_2} (\sin^4 \alpha + \cos^4 \alpha) + \frac{\sin^2 2\alpha}{4} \left( \frac{1}{E_1} + \frac{1}{E_2} - \frac{1}{G_2} \right), \\ S_{33} &= \frac{1}{E_1} \sin^4 \alpha + \frac{1}{E_2} \cos^4 \alpha + \frac{\sin^2 2\alpha}{4} \left( \frac{1}{G_2} - \frac{2\mu_2}{E_2} \right), \\ S_{35} &= \left[ \frac{1}{E_2} \cos^2 \alpha - \frac{1}{E_1} \sin^2 \alpha + \left( \frac{\mu_2}{E_2} - \frac{1}{2G_2} \right) \cos 2\alpha \right] \sin 2\alpha. \end{aligned}$$

## Elastic parameters test

The uniaxial compression test was performed on a set of samples with bedding angle  $\alpha$  of  $0^\circ$ ,  $45^\circ$  and  $90^\circ$ . Four elastic parameters can be measured based on the relationship between stress and strain.

(1) When the bedding inclination angle  $\alpha=0^\circ$ , the stress-strain relationship can be given

$$\begin{cases} \frac{\varepsilon_x}{\sigma_z} = -\frac{\mu_2}{E_2} \\ \frac{\varepsilon_y}{\sigma_z} = -\frac{\mu_2}{E_2} \\ \frac{\varepsilon_z}{\sigma_z} = \frac{1}{E_2} \end{cases} \quad (6)$$

According to equation (6) and the uniaxial compression test of the sample with the bedding angle  $\alpha=0^\circ$ , the elastic modulus  $E_2$  and poisson's ratio  $\mu_2$  perpendicular to the direction of the bedding plane can be obtained.

(2) When the bedding angle  $\alpha=90^\circ$ , the stress-strain relationship can be given

$$\begin{cases} \frac{\varepsilon_x}{\sigma_z} = -\frac{\mu_1}{E_1} \\ \frac{\varepsilon_y}{\sigma_z} = -\frac{\mu_2}{E_2} \\ \frac{\varepsilon_z}{\sigma_z} = \frac{1}{E_1} \end{cases} \quad (7)$$

According to equation (7) and the uniaxial compression test of the sample with the bedding angle  $\alpha=90^\circ$ , the elastic modulus  $E_1$  and poisson's ratio  $\mu_1$  parallel to the direction of the bedding plane can be obtained.

(3) When the bedding angle  $\alpha=45^\circ$ , the stress-strain relationship can be given

$$\begin{cases} \frac{\varepsilon_x}{\sigma_z} = -\frac{1}{2} \left( \frac{\mu_1}{E_1} + \frac{\mu_2}{E_2} \right) \\ \frac{\varepsilon_y}{\sigma_z} = \frac{1}{4} \left( \frac{1}{E_1} + \frac{1}{E_2} - \frac{1}{G_2} \right) - \frac{1}{2} \frac{\mu_2}{E_2} \\ \frac{\varepsilon_z}{\sigma_z} = \frac{1}{4} \left( \frac{1}{E_1} + \frac{1}{E_2} + \frac{1}{G_2} - \frac{2\mu_2}{E_2} \right) \end{cases} \quad (8)$$

According to equation (8), the uniaxial compression test is performed on the sample with the bedding angle  $\alpha=45^\circ$ , combined with equations (6) and (7), the  $E_1$ ,  $\mu_1$ ,  $E_2$ , and  $\mu_2$  of the bedding angle can be solved.

## Experiment process

### Experiment material

The rock samples used in the test were all collected from the carbonaceous slate on the slope of the

tailing pond of the Pulang copper mine in Shangri-La, Yunnan, China. The rock blocks were processed into a diameter of 50mm and a height of the 100mm standard rock sample is shown in Figure 2. The bedding angle  $\alpha$  is defined as the angle between minor principal direction and planes of anisotropy. The physical parameters of carbonaceous slate were obtained through standard tests, and the results are listed in Table 1.



**Fig. 2** Layered carbonaceous slate sample core and standard rock sample

**Table 1** Rock mass strength parameters

Rock Types	Porosity(%)	Unit Weight ( $\text{kN/m}^3$ )	Cohesion ( $\text{kPa}$ )	Friction Angle( $^\circ$ )
Carbonaceous slate	3.54	22.4	93.6	33.3

## Test procedure

In the experiment, 12 pieces of carbonaceous slate with different bedding inclination angles ( $\alpha=0^\circ$ ,  $15^\circ$ ,  $30^\circ$ ,  $45^\circ$ ,  $60^\circ$ ,  $75^\circ$  and  $90^\circ$ ) were selected, divided into 6 groups, 6 groups corresponding to 6 kinds of freezing and thawing Cycle times (0, 5, 10, 15, 20 and 25), a total of 84 rock samples. Divide the samples with different bedding angles into 6 groups. The first group is to test without freezing and thawing. The second, third, fourth, fifth and sixth groups were tested under 5, 10, 15, 20 and 25 freeze-thaw cycles. Perform uniaxial compression tests on the rock samples that have completed the freeze-thaw cycle test in sequence.

## Freeze-thaw cycle test

Place the sample in an electric oven to dry, and cool the sample to room temperature after 24 hours. Then use a vacuum collector for vacuum saturation. Place the saturated sample at  $-20^\circ\text{C}$  for 12 hours. The sample was then immersed in water at  $20^\circ\text{C}$  for 12 hours. Thus, each freeze-thaw cycle lasts for 24 hours, as shown in Figure 3. The compressive strength of the sample was measured after 0, 5, 10, 15, 20 and 25 cycles.

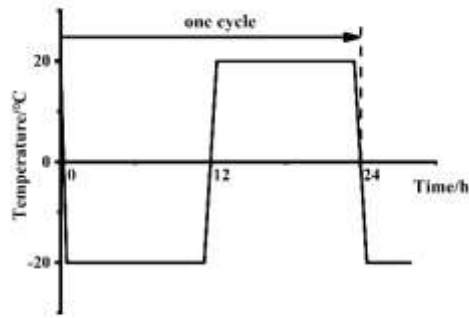


**Fig. 3** The temperature control curve for each freeze-thaw cycle

### Experimental procedures for compression experiments

After undergoing different numbers of freeze-thaw cycles, samples with different bedding angles were subjected to uniaxial compressive strength experiments. The experiment uses a pressure testing machine (THY-2000 electro-hydraulic pressure testing machine), a strain data acquisition instrument (YE2538A static strain gauge) and a PC terminal, as shown in Figure 4. The maximum load of the testing machine is 100kN, the force measurement accuracy is  $\pm 0.5\%$ , and the displacement resolution is 0.001mm. The test loading rate is 0.2mpa/s, until the sample is broken, the stress-strain curve is automatically collected by the data acquisition system.



**Fig. 4** Uniaxial compression test instrument

## Deterioration analysis of mechanical parameters

### Mechanical parameter analysis

The stress-strain curves of carbonaceous slate samples with different bedding dip angles after 0, 5, 10, 15, 20, and 25 freeze-thaw cycles are shown in Figure 5. The stress-strain curve of this test consists of three parts: compression microcracks, elastic deformation and crack expansion. It can be found that the stress-strain curves of the six groups of samples are similar in shape. And as the number of freeze-thaw cycles increases, the general trend of strain decreases. It is worth noting that the minimum slope of the curve is concentrated at 30°, 45° and 60°.

The elastic modulus, poisson's ratio and uniaxial compressive strength values of carbonaceous slate

are shown in Figure 6. With the increase of the number of freeze-thaw cycles, the elastic modulus and uniaxial compressive strength of carbonaceous slate gradually decrease, while the poisson's ratio gradually increases. In addition, as the bedding angle of the sample increases, the elastic modulus and uniaxial compressive strength first decrease and then increase, while the poisson's ratio first increases and then decreases. It is worth noting that the minimum values of elastic modulus and uniaxial compressive strength and the maximum value of poisson's ratio obtained from each group of experiments are concentrated at  $\alpha=30^\circ$ ,  $45^\circ$  and  $60^\circ$ , and the slope of the stress-strain curve is the smallest. The value corresponds. The above experimental results show that freezing and thawing will cause the structural damage of carbonaceous slate, and will affect the mechanical parameters of the rock together with the bedding dip angle of the rock, especially when the bedding dip at  $\alpha=30^\circ$ ,  $45^\circ$  and  $60^\circ$ .

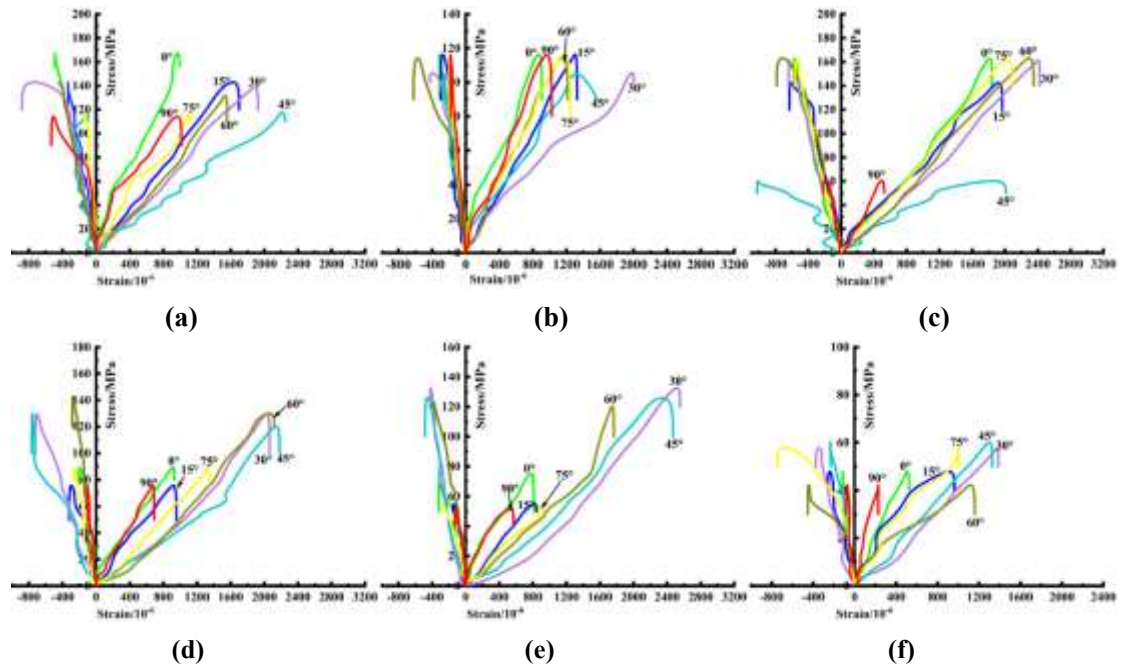


**Fig. 5** Stress-strain curves of layered rocks after different freeze-thaw cycles: **a** 0 freeze-thaw cycles, **b** 5 freeze-thaw cycles, **c** 10 freeze-thaw cycles, **d** 15 freeze-thaw cycles, **e** 20 freeze-thaw cycles, **f** 25 freeze-thaw cycles

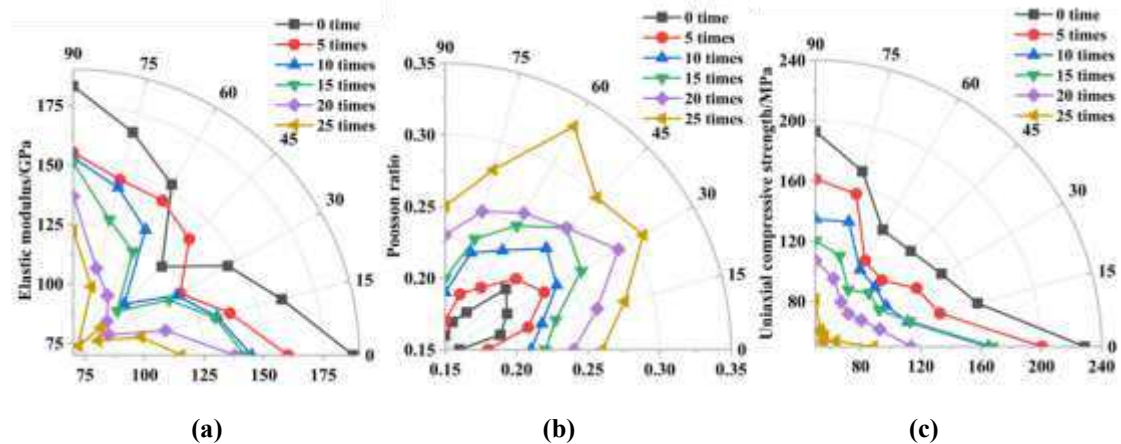


**Fig. 6** Variety in mechanical parameters of layered rocks: **a** elastic modulus, **b** poisson's ratio, **c** uniaxial compressive strength

## **Deterioration of rock mechanical parameters**

Under freezing conditions, the pores in the rock will freeze, causing the rock to expand and increase in volume. The force generated by the volume expansion of the rock acts on the rock pore wall, and this force easily exceeds the tensile strength limit of the rock pore wall, leading to the development and extension of rock cracks and even failure. At the same time, due to the different bedding angles of the rocks, the limits of the forces that the rocks can bear are different. (Liu et al. 2015)

As the results of this experimental study show, as the freeze-thaw cycle increases, the uniaxial compressive strength of the rock gradually decreases, and the degree of rock damage gradually increases. This is because temperature changes during freezing and thawing lead to changes in the internal stress of the rock, leading to an increase in pore volume (Monteiro et al. 1985; Hori and Morihiro 1998). The compressive strength and elastic modulus of the rock also decrease (Ince and Fener 2016). And as the bedding inclination increases, the limit of the force that the rock can withstand first decreases and then increases. This is because under the influence of repeated freezing and thawing cycles, the anisotropy of the rock and the thermal expansion rate of the particles will change, causing the binding force between the particles to also change, forming cracks of different shapes (Chen et al. 2000), Eventually lead to failure of the sample. During the freeze-thaw cycle, the sample undergoes these two types of degradation: crack expansion and particle degradation.

## **Numerical modeling**

### **Overview of Numerical Models**

The study in this paper is a layered rock slope in the Pulang copper mine area in Yunnan, China, as shown in Figure 7, and uses the indoor freeze-thaw test data to analyze the deformation characteristics and stability of carbonaceous slate slopes with different bedding dips before and after the freeze-thaw cycle. The freezing period of Pulang Copper Mine can last about five months, so the time selected for this simulation is 154 days. Using finite element software to build a numerical model of the slope. The height of the slope model is 89m and the length is 217m. The grid size of the shallow area is set to 1m, and the grid size of the deep area is set to 5m. The grid model is divided into 7057 nodes and 6960 units. In order to study the characteristics of different locations, 3 monitoring lines and 3 monitoring points were set up on  $x=25\text{m}$  (top of slope),  $x=67\text{m}$  (middle of slope) and  $x=108\text{m}$  (toe of slope). The boundary of the model is constrained at the bottom, AC and FH are at zero displacement, and CD is a free surface.

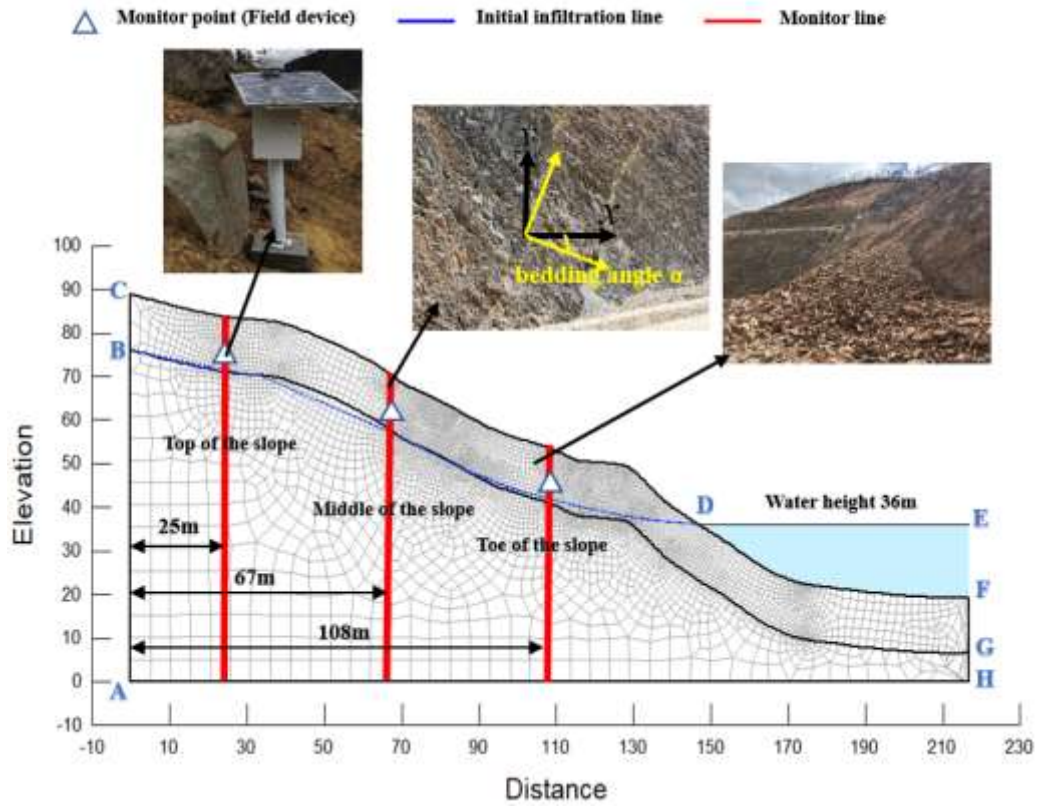


Fig. 7 Grid model

## Safety factor of layered rock slope

In this study, the Morgenstern-Price method based on limit equilibrium theory was used to calculate the safety factor of the slope. This method can determine the relevant parameters more accurately by studying the sliding surface of rock landslides under the limit equilibrium state, and provides a reliable basis for the analysis and design of landslide engineering (Morgenstern and Price 1965). Therefore, it is more reasonable to use the Morgenstern-Price method in slope stability analysis (Xiao and Li 2020). And the improved method satisfies force balance and torque balance, and the calculation accuracy is higher.

Taking the rock slice as the research object, as shown in Figure 8, when the boundary conditions  $E_0 = 0$  and  $E_n = 0$ , according to the balance of the force in the normal and tangential directions of the slip surface of the rock slice, it can be obtained:

$$S_i = (N_i \tan \varphi + cb \sec \alpha) / F_s \quad (9)$$

$$N_i = (W_i + \lambda f_{i-1} E_{i-1} - \lambda f_i E_i + Q_i \cos \omega_i + J_i \sin \beta_i) \cos \alpha + E_i - E_{i-1} + Q_i \sin \omega_i - J_i \cos \beta_i \sin \alpha \quad (10)$$

where  $N_i$  is the effective normal force on the slip surface of the rock slice and the unit is kN;  $S_i$  is the shear force on the slip surface of the rock slice and the unit is kN, and the safety factor  $F_s$  can be derived as:

$$F_s = \frac{\sum_{i=1}^{n-1} (R_i \prod_{j=i}^{n-1} \psi_j) + R_n}{\sum_{i=1}^{n-1} (T_i \prod_{j=i}^{n-1} \psi_j) + T_n} \quad (11)$$

where  $R_i$  is the resistance force,  $R_i = [W_i \cos \alpha_i + Q_i \cos(\omega_i - \alpha_i) + J_i \sin(\beta_i - \alpha_i)] \tan \varphi_i + c_i b_i \sec \alpha_i$  and the unit is kPa;  $T_i$  is the sliding force,  $T_i = W_i \sin \alpha - Q_i \sin(\omega_i - \alpha_i) + J_i \cos(\beta_i - \alpha_i)$ ;  $\psi_i$  is the transfer coefficient,  $\psi_{i-1} = \frac{(\sin \alpha_i - \lambda f_{i-1} \cos \alpha_i) \tan \varphi_i + (\cos \alpha_i + \lambda f_{i-1} \sin \alpha_i) F_s}{(\sin \alpha_{i-1} - \lambda f_{i-1} \cos \alpha_{i-1}) \tan \varphi_{i-1} + (\cos \alpha_{i-1} + \lambda f_{i-1} \sin \alpha_{i-1}) F_s}$ ;  $c_i$  is the effective cohesion for every rock slice and the unit is kPa;  $\varphi_i$  represents the shear strength angle for every rock slice, the unit is the degree.  $J_i$  is the seepage force of the rock slip which adopts a simplified seepage field treatment method, assuming that its position of action is located at the center of gravity of the rock below the underwater line, and the distance from the center of the slip surface of the rock strip is  $h_{wi}/2$ , and  $h_{wi}$  is the distance from the underwater line to the slip surface.  $E_i$  and  $E_{i-1}$  are the horizontal effective forces between the two sides of the rock slice and the unit is kN;  $\lambda f_i E_i$  and  $\lambda f_{i-1} E_{i-1}$  are the shear forces between the two sides of the rock strip,  $f_i$  is the function of the inter-strip force, and  $\lambda$  is the proportional coefficient. The distances between the action positions on both sides and the center of the slip surface of the rock strip are  $Z_i$  and  $Z_{i-1}$ , respectively;  $W_i$  is divided into two parts based on the underwater line:  $W_i = W_{i1} + W_{i2}$ , where  $W_{i1}$  is the gravity of the rock above the underwater line and  $W_{i2}$  is floating weight of the rock below the underwater line.  $Q_i$  is an external force on the rock surface;  $\omega_i$  is the angle between the direction of the external force and the normal direction;  $\alpha_i$  is the angle of the slip surface.

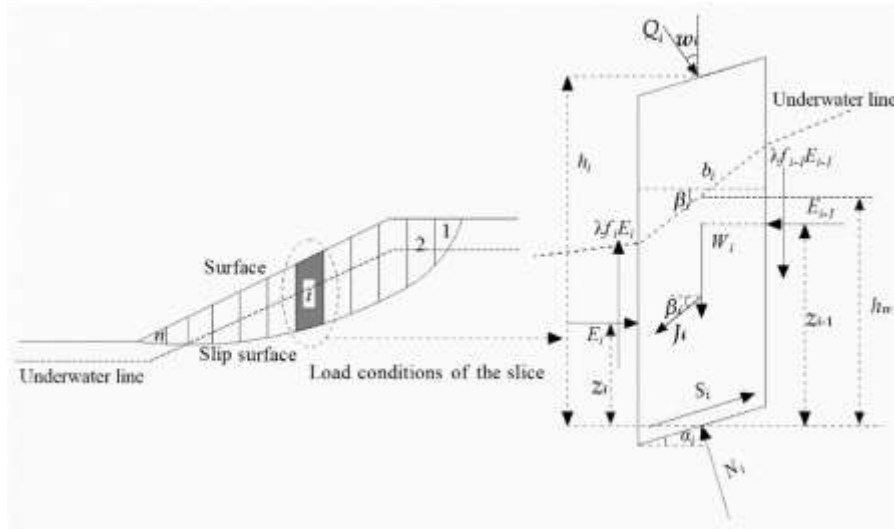


**Fig. 8** Morgenstern–Price (M–P) method calculation principle and model (Xia CZ et al. 2020)

## Discussion

### Influence of bedding dip on horizontal displacement of carbonaceous slate slope

The layered rock mass will produce corresponding displacement under the effect of freezing and thawing. Therefore, according to the calculation conditions and experimental data in Table 1, a total of 42 times value simulations were performed, and 252 horizontal displacement (HD) distributions were obtained. In order to highlight the influence of the number of freeze-thaw cycles and the bedding inclination angle on the horizontal displacement, 0 freeze-thaw cycles, 10 freeze-thaw cycles and 20 freeze-thaw cycles are selected to illustrate the influence of the bedding inclination angle on the deformation characteristics. The horizontal displacements of  $\alpha=0^\circ$ ,  $45^\circ$  and  $90^\circ$  under different freeze-

thaw cycles are shown in Figure 9 to illustrate the influence of different freeze-thaw cycles on the deformation characteristics.

In Figure 9, the horizontal displacement under 0 freeze-thaw cycle is the horizontal displacement distribution of the slope before the freeze-thaw cycle begins, and the rest is the horizontal displacement distribution of the slope after 10 and 20 freeze-thaw cycles of the layered rock mass. For the top, middle and toe of the slope, the horizontal displacement gradually increases with the increase of the height, and first increases and then decreases with the increase of the bedding dip. The maximum horizontal displacement occurs near the surface of the slope. It is worth noting that when the inclination of the rock formation reaches  $45^\circ$ , the horizontal displacement of all positions reaches the maximum. It may be due to the fact that when the dip angle of the carbonaceous slate reaches  $45^\circ$ , the carbonaceous slate has a larger porosity. Under low temperature freezing, the pore water or fissure water in the carbonaceous slate will freeze into ice and cause greater porosity. The volume expansion rate produces a large tensile stress inside it, causing internal cracks to expand. Therefore, ignoring the layer dip in the study of layered rock slopes may underestimate the horizontal displacement.

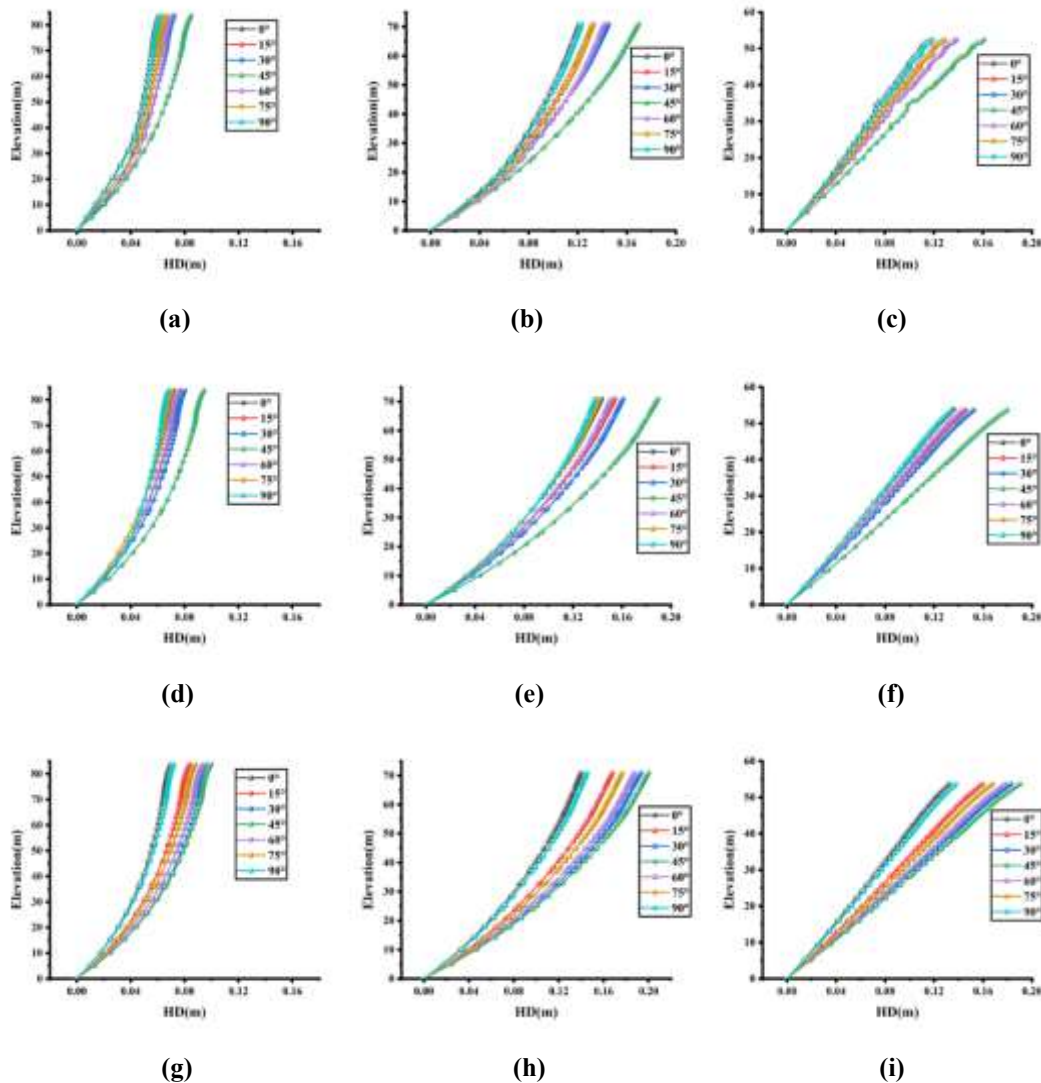


**Fig. 9** Variations of horizontal displacement under different freeze-thaw cycles for layered rock slope: **a** top of the slope with 0 freeze-thaw cycle, **b** middle of the slope with 0 freeze-thaw cycle, **c** toe of the

slope with 0 freeze-thaw cycle, **d** top of the slope with 10 freeze-thaw cycles, **e** middle of the slope with 10 freeze-thaw cycles, **f** toe of the slope with 10 freeze-thaw cycles, **g** top of the slope with 20 freeze-thaw cycles, **h** middle of the slope with 20 freeze-thaw cycles, **i** toe of the slope with 20 freeze-thaw cycles

### The influence of the number of freeze-thaw cycles on the horizontal displacement of the carbonaceous slate slope

The trend of horizontal displacement changes in Figure 10 is similar to Figure 9. The horizontal displacement of carbonaceous slate slopes with different bedding dip angles increases with the increase in the number of freeze-thaw cycles. This is in line with the experimental results. As the number of freeze-thaw cycles increases, the degree of freeze-thaw damage of layered rocks increases, which ultimately leads to an increase in the deformation of the carbonaceous slate slope. Compared with the top of the slope, the horizontal displacement values of the middle part of the slope and the foot of the slope are larger, because it is close to the tailings reservoir water. Therefore, during the freeze-thaw cycle, the probability of landslides in the middle of the slope and the toe is greater than that at the top of the slope.

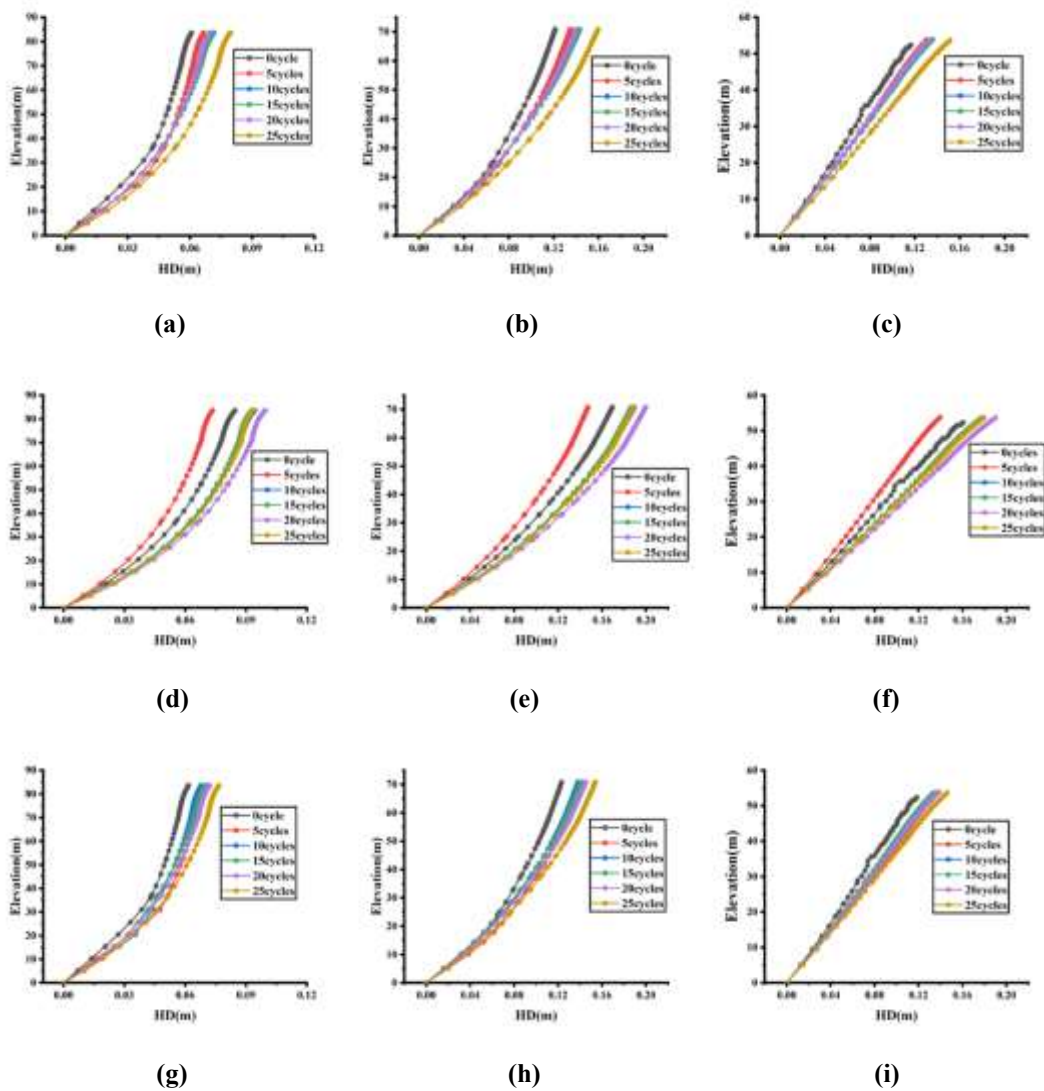


**Fig. 10** Variations of horizontal displacement under different  $\alpha$  values for layered rock slope: **a** top of the slope with  $\alpha=0^\circ$ , **b** middle of the slope with  $\alpha=0^\circ$ , **c** toe of the slope with  $\alpha=0^\circ$ , **d** top of the slope with  $\alpha=45^\circ$ , **e** middle of the slope with  $\alpha=45^\circ$ , **f** toe of the slope with  $\alpha=45^\circ$ , **g** top of the slope with  $\alpha=90^\circ$ , **h** middle of the slope with  $\alpha=90^\circ$ , **i** toe of the slope with  $\alpha=90^\circ$

### Analysis of Maximum Horizontal Displacement of Stratified Rock Slope

In order to more prominently study the deformation of different positions of the slope under different freeze-thaw cycles and rock inclination conditions, the concept of maximum horizontal displacement (MHD) of the slope is defined. As shown in Figure 11(a)-(c), the maximum horizontal displacement at different positions of the slope is greatly affected by the number of freeze-thaw cycles and the inclination of the rock formation. When  $\alpha=45^\circ$ , MHD reaches its maximum value. In this case, the elastic modulus and Poisson's ratio of the rock slope are both small. When  $\alpha$  is close to  $0^\circ$  or  $90^\circ$ , MHD reaches its minimum value. Previous studies only considered the number of freeze-thaw cycles or the dip angle of the rock formation, but ignored their combined effects. Table 2 shows that for the judgment standard of MHD, only the number of freeze-thaw cycles or rock inclination is considered and the difference between the number of freeze-thaw cycles and rock inclination is considered at the same time. It can be seen from the table below that when only the number of freeze-thaw cycles or  $\alpha$  is considered and the number of freeze-thaw cycles and  $\alpha$  are considered at the same time, the MHD values of carbonaceous slate slopes are quite different. Therefore, the number of freeze-thaw cycles and the layer dip angle  $\alpha$  must be considered in the deformation analysis of rock slopes.

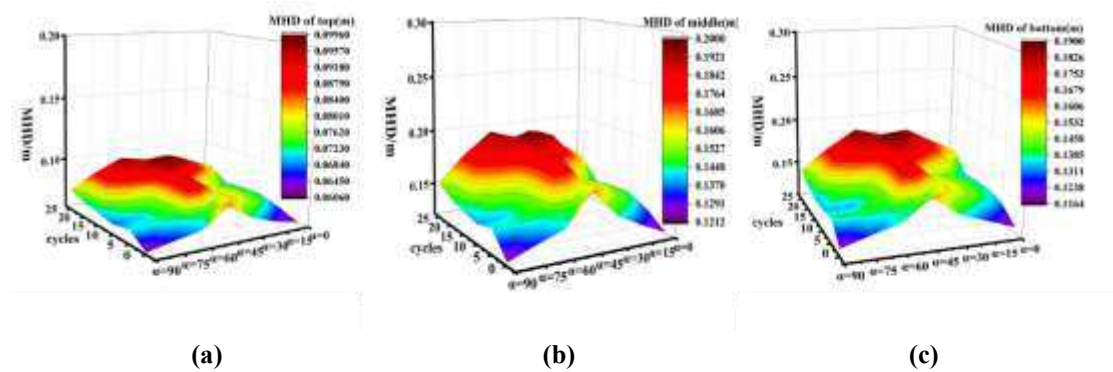


**Fig. 11** Variations of maximum horizontal displacement (MHD) under different freeze-thaw cycles  $\alpha$  values for layered rock slope: **a** top of the slope, **b** middle of the slope, **c** toe of the slope

**Table 2** Only considering the number of freeze-thaw cycles or  $\alpha$ , and considering the difference between the number of freeze-thaw cycles and  $\alpha$  at the same time

MHD	Only considering the number of freeze-thaw cycles	Only considering bedding dip $\alpha$	Considering both freeze-thaw cycles and bedding dip $\alpha$
Top of slope	23.5%	24.05%	28.6%
Middle of slope	25.8%	26.3%	33.4%
Toe of slope	24%	22.8%	38.8%

## Freeze-thaw cycles and bedding dips affect the stability of lower layered rock slopes

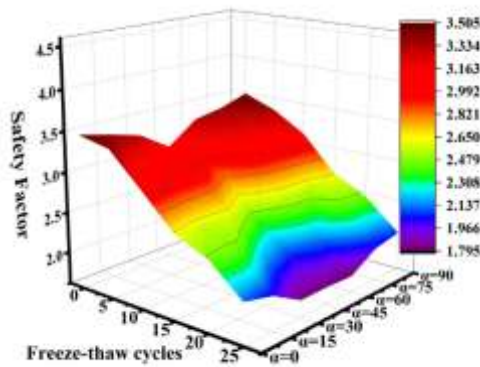


Fig. 12 Variation of SF for layered rock slope

Figure 12 shows the changes in the safety factor (SF) of the carbonaceous slate slope under different freeze-thaw cycles and bedding dip  $\alpha$ . It can be seen that the freeze-thaw cycle and the bedding dip have a significant impact on the stability of the slope. After 25 freeze-thaw cycles, the safety factor dropped from 3.501 to 1.796, and the degradation effect of the freeze-thaw cycle is obvious. Generally speaking, the safety factor of mine rock slopes between 1.1-1.3 (Yu RC 2009) means that the slope is stable. In this numerical simulation, even after 25 freeze-thaw cycles, the safety factor of the slope is still 1.796, which is higher than the normal design value. This is because, according to the freezing and thawing mechanism of the rock, the slope initially undergoes a degradation effect on the surface and gradually deepens. After 25 freeze-thaw cycles, the freeze-thaw cycle still mainly affects the shallow rock mass of the slope, while the internal layered rock is only slightly degraded. When the freeze-thaw cycle is constant, the safety factor of the slope first decreases and then increases with the increase of the carbonaceous slate bedding dip. It is worth noting that, because the deformation characteristics of the slope change the most when the bedding dip is  $45^\circ$ , the safety factor of the carbonaceous slate slope is the smallest at  $45^\circ$ .

## Conclusion

Through a series of indoor freeze-thaw tests and uniaxial compression tests, the effects of freeze-thaw cycles and bedding dips on the elastic parameters and uniaxial compressive strength of layered rocks are studied. This study provides a basis for geotechnical engineering in cold regions. The main conclusions are as follows:

- Through laboratory tests, it is found that the elastic modulus and uniaxial compressive strength of carbonaceous slate gradually decrease with the increase of the number of freeze-thaw cycles, while the Poisson's ratio gradually increases. In addition, the elastic modulus and uniaxial compressive strength first decrease and then increase with the increase of the bedding angle of the sample, while the Poisson's ratio first increases and then decreases. Especially when the bedding dip angle  $\alpha=30^\circ$ ,  $45^\circ$  and  $60^\circ$ , the impact on the carbonaceous slate is most obvious.
- The study found that the number of freeze-thaw cycles and the bedding inclination will have a greater impact on the deformation characteristics of layered rock slopes. As the number of freeze-

thaw cycles increases, the degree of freeze-thaw damage of layered rocks increases, which ultimately results in layered rock quality. The deformation of the slope increases. In addition, the horizontal displacement first increases and then decreases with the increase of the bedding inclination angle, and reaches the maximum value when the bedding inclination angle  $\alpha=45^\circ$ , which corresponds to the results obtained from the indoor test.

- The maximum horizontal displacement (MHD) is defined to reflect the deformation characteristics of the layered rock slope. When  $\alpha=45^\circ$ , the MHD reaches the maximum, and when  $\alpha$  is close to  $0^\circ$  or  $90^\circ$ , the MHD reaches the minimum. In addition, the number of freeze-thaw cycles and the layer dip angle  $\alpha$  must be considered in the deformation analysis of rock slopes.
- During the freeze-thaw cycle, the quality strength of the layered rock slope gradually decreases, and the safety factor also gradually decreases. In addition, the safety factor of the slope first decreases and then increases with the increase of the bedding inclination. When the bedding inclination angle  $\alpha=45^\circ$ , the safety factor reaches the minimum. Therefore, the use of numerical simulation to analyze slope stability in cold areas is helpful to identify potentially dangerous areas of slopes. At the same time, it is necessary to formulate prevention and control measures according to the actual situation of the bedding dip of the layered rock slope in cold areas to ensure the stability of the layered rock slope.

**Author contribution** Guangkeng Zhang wrote the manuscript, completed the experiment and method design, analyzed the data, and performed the experiments. Guangyin Lu and Chengzhi Xia helped provide analysis of raw data. Lianrong Wu, Zhipeng Li and Baosheng Shi helped polish the manuscript. Guangyin Lu provided research funding. Huiyun Wang and Jinxi Wei changed the format of the manuscript. All authors have read and agreed to the published version of the manuscript.

**Funding** This work was supported by the National Natural Science Foundation of China (No.41974148), the Key R&D Program of Hunan Province of China (No.2020SK2135), the Natural Resources Research Project of Hunan Province of China (No.2021-15) and the Science and Technology Project of Hunan Provincial Department of Transportation (No.202012).

**Availability of data and material** The datasets used or analyzed during the current study are available from the corresponding author on reasonable request.

## Declarations

**Conflict of interest** The authors declare that they have no conflicts of interest.

## References

- Amadei B (1996) Importance of anisotropy when estimating and measuring in situ stresses in rock. *International Journal of Rock Mechanics & Mining Sciences* 33(3):293–325
- Arosio D, Longoni L, Mazza F, Papini M, Zanzi L (2013) Freeze-thaw cycles and rockfall monitoring. *Landslide Sci Pract* 2:385–390
- Chen Q, Nezhad MM, Fisher Q, Zhu HH (2016) Multi-scale approach for modeling the transversely isotropic elastic properties of shale considering multi-inclusions and interfacial transition zone.

- Chen TC, Mori N, Suzuki T, Shoji H, Goto T (2000) Experimental study on crack development of rock specimens by freezing and thawing cycles. *J Jpn Geotech Soc Soils Found* 40(2): 41–48
- Chen YL, Ni J, Jiang LH, Liu ML, Wang P, Azzam R (2014) Experimental study on mechanical properties of granite after freeze-thaw cycling. *Environ Earth Sci* 71(8):3349–3354
- Fu HL, Zhang JB, Huang Z, Shi Y, Wang J (2019) Experimental investigations on the elastic parameters and uniaxial compressive strength of slate under freeze–thaw cycles. *Geomechanics and Geoengineering* 14(4):285–296
- Hori M, Morihiro H (1998) Micromechanical analysis of deterioration due to freezing and thawing in porous brittle materials. *Int J Eng Sci* 36(4):11–522
- Ince I, Fener M (2016) A prediction model for uniaxial compressive strength of deteriorated pyroclastic rocks due to freeze–thaw cycle. *J Afr Earth Sci* 120:134–140
- Ismail I, Mustafa F, (2016) A prediction model for uniaxial compressive strength of deteriorated pyroclastic rocks due to freeze–thaw cycle. *Journal of African Earth Sciences* 120:34–140
- Korshunov AA, Doroshenko SP, Nevzorov AL (2016) The impact of freezing–thawing process on slope stability of earth structure in cold climate. *Procd Eng* 143:682–688
- Li JL, Zhu LY, Zhou KP, Chen H, Shen YJ (2021) Non-linear creep damage model of sandstone under freeze-thaw cycle. *Journal of Central South University* 28(3):954–967
- Li N, Chen GD, Xie DY (2001) Geomechanics development in civil construction in Western China. *Chin J Geotech Eng* 23(03):268–272
- Liu QS, Huang SB, Kang YS, Cui XZ (2015) Advance and review on freezing–thawing damage of fractured rock. *Chin J Rock Mech Eng* 34(03):452–471
- Mokhtari M, Schipper DJ, Vleugels N, Noordermeer JWM (2016) Transversely isotropic viscoelastic materials: contact mechanics and friction. *Tribology International* 97:116–123
- Monteiro PJM, Bastacky SJ, Hayes TL (1985) Low-temperature scanning electron microscope analysis of the Portland cement paste early hydration. *Cem Concr Res* 15(4):687–693
- Morgenstern NR, Price VE (1965) The Analysis of the Stability of General Slip Surfaces. *Géotechnique* 15:79–93
- Qiao GW, Wang YS, Yang XL (2015) Study of rock mass quality evaluation system of freezing–thawing and weathering slopes. *Rock Soil Mech* 36(02):515–522
- Tien YM, Kuo MC (2001) A failure criterion for transversely isotropic rocks. *International Journal of Rock Mechanics and Mining Sciences* 38(3):399–412
- Wen L, Li XB, Yin YB, Gao L (2014) Study of physicomechanical properties of granite porphyry and limestone in slopes of openpit metal mine under freezing–thawing cycles and their application. *J Glaciol Geocryol* 36(3):632–639
- Wu ZW, Liu YZ (2005) Frozen soil foundation and architectural projects. China Ocean Press, Beijing
- Xia CZ, Lu GY, Zhu ZQ, Wu LR, Zhang L, Luo S, Dong J (2020) Deformation and Stability Characteristics of Layered Rock Slope Affected by Rainfall Based on Anisotropy of Strength and Hydraulic Conductivity. *Water* 12(11):3056
- Xiao YY, Li AR (2020) Change of Soft Rock Slope Stability with Weak Interlayer under Rainfall Conditions. *Journal of Yibin University* 20(12):16–19
- Yan XD, Liu HY, Xing CF, Li C, Wang DH (2015) Constitutive model research on freezing–thawing damage of rock based on deformation and propagation of microcracks. *Rock Soil Mech* 36(12):3489–3499

Yu RC (2009) Mining engineer's handbook. Metallurgical Industry Press, Beijing

Zwissler B, Oommen T, Vitton S (2014) A study of the impacts of freeze–thaw on cliff recession at the calvert cliffs in calvert county, Maryland. Geotech Geol Eng 32(4):1133–1148